



We use averaging and homogenization theory to study the propagation of traveling pulses in an inhomogeneous excitable neural network. The network is modeled in terms of a nonlocal integro-differential equation, in which the integral kernel represents the spatial distribution of synaptic weights. We show how a spatially periodic modulation of homogeneous synaptic connections leads to an effective reduction in the speed of a traveling pulse. In the case of large amplitude modulations, the traveling pulse represents the envelope of a multibump solution, in which individual bumps are nonpropagating and transient. The appearance (disappearance) of bumps at the leading (trailing) edge of the pulse generates the coherent propagation of the pulse. Wave propagation failure occurs when activity is insufficient to maintain bumps at the leading edge.

traveling waves, excitatory neural network, inhomogeneous media, homogenization, neural field theory, wave propagation failure

92C20

10.1137/070699214

Traveling waves of electrical activity have been observed in vivo in a number of sensory cortical areas including the somatosensory cortex of behaving rats [30], turtle and mollusk olfactory bulbs [22, 23], turtle cortex [34], and visuomotor cortices in the cat [36]. Such waves are usually seen during periods without sensory stimulation; the subsequent presentation of a stimulus then induces a switch to synchronous oscillatory behavior [13]. Traveling waves are also a characteristic feature of certain neurological disorders in humans, including epilepsy [8] and migraines [24]. Therefore, investigating the mechanisms underlying wave propagation in neural tissue is important for understanding both normal and

Mathematical analyses of cortical wave propagation typically consider reduced one-dimensional network models. Under the additional assumption that the synaptic interactions are homogeneous, it has been shown that an excitatory neural network supports the propagation of a traveling front [12, 19, 5] or, in the presence of slow adaptation, a traveling pulse [39, 1, 31, 42, 43, 10, 11, 14, 38]. However, the patchy nature of long-range horizontal connections in superficial layers of certain cortical areas suggests that the cortex is more realistically modeled as an inhomogeneous neural medium. For example, in the primary visual cortex the horizontal connections tend to link cells with similar stimulus feature preferences such as orientation and ocular dominance [28, 41, 2]. Moreover, these patchy connections tend to be anisotropic, with the direction of anisotropy correlated with the underlying orientation preference map. Hence the anisotropic pattern of connections rotates approximately periodically across the cortex resulting in a periodic inhomogeneous medium [3, 4]. Another example of inhomogeneous horizontal connections is found in the prefrontal cortex [27, 29, 17], where pyramidal cells are segregated into stripes that are mutually connected via horizontally projecting axon collaterals; neurons within the gaps between stripes do not have such projections.

In this paper we investigate how a spatially periodic modulation of long-range synaptic weights affects the propagation of traveling pulses in a one-dimensional excitatory neural network, extending previous work on traveling fronts in neural network models [3] and reaction-diffusion systems [20, 21]. We proceed by introducing a slowly varying phase into the traveling wave solution of the unperturbed homogeneous network, and then we use perturbation theory to derive a dynamical equation for the phase, from which the mean speed of the wave can be calculated. We show that a periodic modulation of the long-range connections slows down the wave, and if the amplitude and wavelength of the periodic modulation is sufficiently large, then wave propagation failure can occur. A particularly interesting result of our analysis is that in the case of large amplitude modulations, the traveling pulse is no longer superthreshold everywhere within its interior, even though it still propagates as a coherent solitary wave. We find that the pulse now corresponds to the envelope of a multibump solution, in which individual bumps are nonpropagating and transient. The appearance (disappearance) of bumps at the leading (trailing) edge of the pulse generates the propagation of activity; propagation

(2.2)

$$f(u) = \frac{1}{1 + e^{-\mu u}},$$

where μ is a gain parameter and θ is a threshold. As $\mu \rightarrow \infty$, $f \rightarrow H$, where $H(u) = \begin{cases} 0, & u \leq \theta \\ 1, & u > \theta \end{cases}$ and

(2.3)

$$[u] = \begin{cases} 0, & u \leq 0, \\ 1, & u > 0. \end{cases}$$

The periodic microstructure of the cortex is incorporated by taking the weight distribution to be of the form [3, 4]

$$(2.4) \quad w(x, x') = W(|x - x'|) \left[1 + \mathcal{D}' \left(\frac{x'}{d} \right) \right],$$

where \mathcal{D} is a 2 π -periodic function and d determines the microscopic length-scale. (We consider the first-order derivative of \mathcal{D} so that the zeroth-order harmonic is explicitly excluded.) It is important to note that (2.4) is a one-dimensional abstraction of the detailed anatomical structure found in the two-dimensional layers of real cortex. (See [6] for a more detailed discussion of cortical models.) However, it captures both the periodic-like nature of long-range connections and possible inhomogeneities arising from the fact that this periodicity is correlated with a fixed set of cortical feature maps.

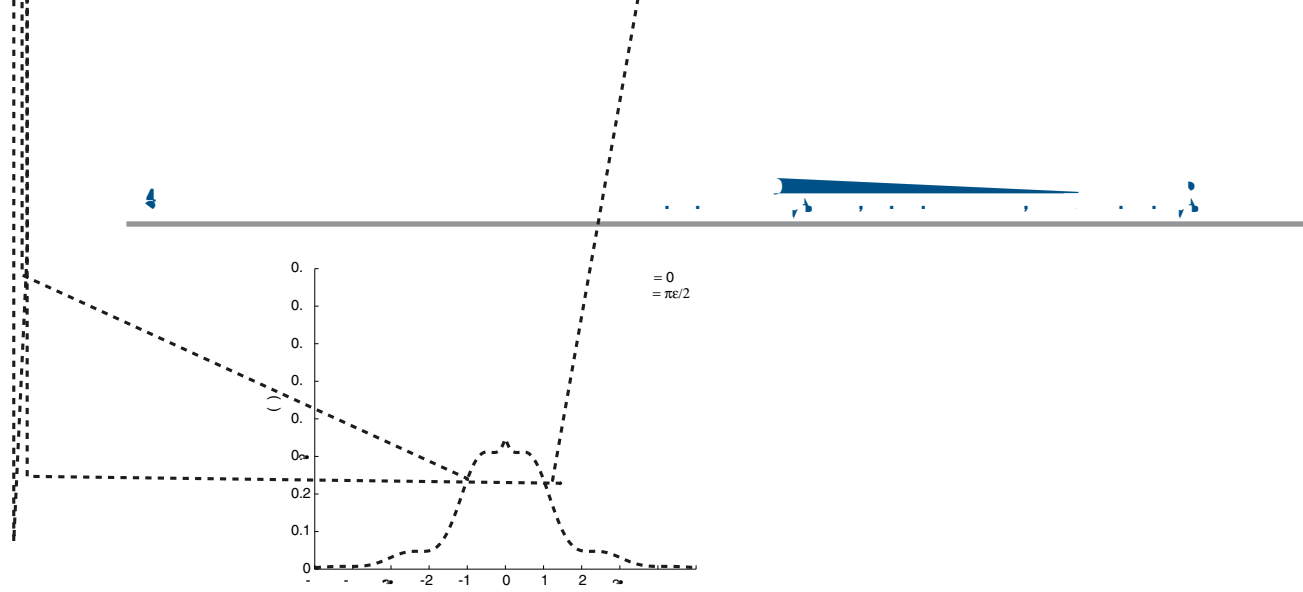
For concreteness, we take the homogeneous weight function W to be an exponential,

$$(2.5) \quad W(x) = \frac{W}{2d} e^{-|x|/d},$$

where d is the effective range of the excitatory weight distribution, and set

$$(2.6) \quad \mathcal{D}(x) = \sin(x), \quad 0 \leq x < 1,$$

where A is the amplitude of the periodic modulation., $A = 34.55 \times 10^{-9}$



Although the inhomogeneous system is not translationally invariant, we can assume that perturbations about the homogeneous system will provide us with nearly translationally invariant solutions [20]. Thus, we perform the change of variables $\xi = x - ct$ and $\tau = t$ so that (3.3) becomes

$$(3.4) \quad \begin{aligned} \frac{u(\xi, \tau)}{D} &= -u(\xi, \tau) + \int_{-\infty}^{\infty} W(\xi - \xi') f(u(\xi', \tau)) d\xi' + \tau \frac{u(\xi, \tau)}{D} \\ &+ \int_{-\infty}^{\infty} \mathcal{D} \frac{u(\xi, \tau)}{D} W'(\xi - \xi') f(u(\xi', \tau)) - W(\xi - \xi') \frac{f(u(\xi', \tau))}{D} d\xi', \\ \frac{1}{D} \frac{v(\xi, \tau)}{D} &= -v(\xi, \tau) + u(\xi, \tau) + \tau \frac{v(\xi, \tau)}{D}. \end{aligned}$$

Next perform the perturbation expansions

$$(3.5) \quad u(\xi, \tau) = U(\xi) + u_1(\xi, \tau) + u_2(\xi, \tau) + \dots,$$

$$(3.6) \quad v(\xi, \tau) = V(\xi) + v_1(\xi, \tau) + v_2(\xi, \tau) + \dots,$$

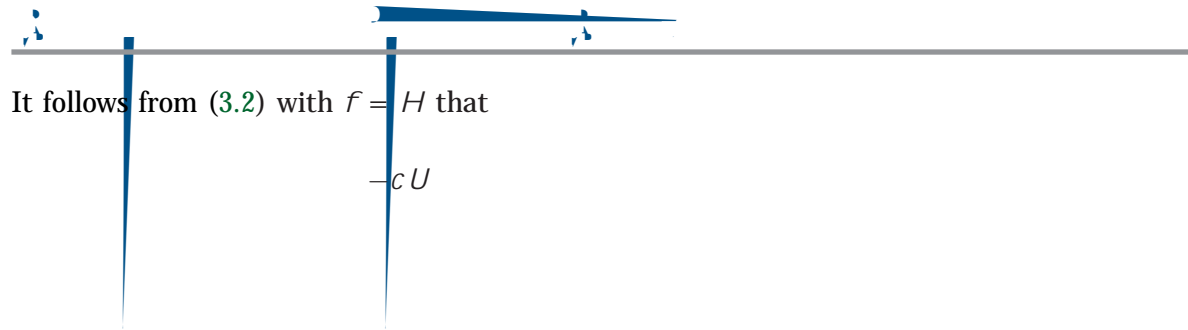
$$(3.7) \quad c(\tau) = c + c_1(\tau) + c_2(\tau) + \dots,$$

where $(U(\xi), V(\xi))$ is a traveling pulse solution of the corresponding homogeneous system (see (3.2)) and c is the speed of the unperturbed pulse. The first-order terms u_1, v_1 satisfy

$$(3.8) \quad -\frac{u_1(\xi, \tau)}{v_1(\xi, \tau)} + \mathcal{L} \frac{u_1(\xi, \tau)}{v_1(\xi, \tau)} = -c_1(\tau) \frac{U'(\xi)}{V'(\xi)} + \frac{h(\xi, -)}{0},$$

where

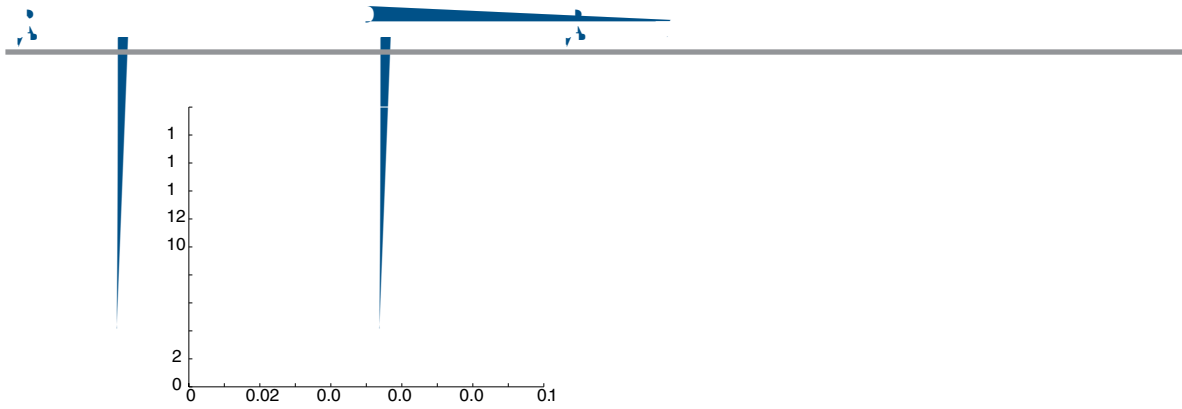
$$(3.9) \quad \mathcal{L} \frac{u}{v} = \frac{c \frac{du}{d\xi} - u}{\frac{c}{D} \frac{dv}{d\xi}} = \frac{c \frac{du}{d\xi} - u + \int_{-\infty}^{\infty} W(\xi - \xi') f'(U(\xi')) u(\xi') d\xi' - v}{\frac{c}{D} \frac{dv}{d\xi}}$$



It follows from (3.2) with $f = H$ that



For



variation in wave speed such that the mean wave speed is approximately independent of ϵ . However, when a pulse enters a region of enhanced synaptic weights, the resulting increase in wave speed coincides with a rapid increase in pulse width as a function of ϵ . Thus, the pulse will tend to extend into neighboring regions of reduced synaptic weights and the resulting spatial averaging will counteract the speeding up of the wave. On the other hand, when a pulse enters a region of reduced synaptic weights, the reduction in wave speed coincides with a reduction in pulse width so that spatial averaging can no longer be carried out as effectively. (The effectiveness of spatial averaging will depend on the ratio of the pulse width a to the periodicity 2π of the weight modulation.) Hence, we expect regions where the weights are reduced to have more effect on wave propagation than regions where the weights are enhanced, suggesting that a periodic weight modulation leads to slower, narrower waves. This is indeed found to be the case, both in our perturbation analysis (section 4.2) and in our numerical simulations (section 5). Interestingly, we also find that traveling waves persist for larger values of ϵ than predicted by our analysis of single bumps in homogeneous networks, although such waves tend to consist of multiple bumps (see section 5).

Suppose that the homogeneous network with a Heaviside nonlinearity supports a stable traveling wave solution (U, ϕ) .

Having found the null-solution (4.14), we now determine the phase function given by (3.16) with $f = H$. First, the constant K of (3.14) is evaluated by substituting for $(A(\cdot), B(\cdot))$ using (4.14) and substituting for $(U(\cdot), V(\cdot))$ using (4.7) and (4.8). The rather lengthy expression for K is given in the appendix. Next, we evaluate the double integral on the right-hand side of (3.16) by setting $D(x) = e^{ix}$ and using Fourier transforms. This gives

$$(4.22) \quad K = \frac{1}{2} \int_{-\infty}^{\infty} W(x) \int_{-\infty}^{\infty} e^{iqx} A^*(q) \widetilde{F(U)}(q + i0) \frac{dq}{2} dx,$$

where $*$ denotes complex conjugate and

$$(4.23) \quad A(q) = \int_{-\infty}^{\infty} e^{iqx} A(x) dx.$$

In the case of a Heaviside nonlinearity and a pulse of width a , $f(U(\cdot)) = (U(\cdot) + a) - (U(\cdot))$, and $A(x)$ is given explicitly by the first component of the null-vector in (4.14). Taking Fourier transforms of these expressions shows that

$$(4.24) \quad A(q) = -1 + \frac{e^{-iqa}}{iq - \mu} + \frac{1}{iq - \mu_-}, \quad \widetilde{F(U)}(q) = \frac{1 - e^{-iqa}}{iq - 0}.$$

If these Fourier transforms are now substituted into (4.22), we have

$$(4.25) \quad K = \frac{1}{2} \int_{-\infty}^{\infty} W(x) \int_{-\infty}^{\infty} \frac{(1 - e^{-iq(a-x)} + e^{iqa} - e^{-ia'}) e^{iqx}}{(q + i0)(q - i\mu)} + \frac{(1 - e^{-iq(a-x)} + e^{iqa} - e^{-ia'}) e^{iqx}}{(q + i0)(q - i\mu_-)} \frac{dq}{2i} dx.$$

The resulting integral over q can be evaluated by closing the contour in the upper-half or lower-half complex q -plane depending on the sign of $x, x \pm a$. We find that there are only contributions from the poles at $q = i\mu_{\pm}$ with $\mu_{\pm} > 0$, whereas there is a removable singularity at $q = -i0$. Thus

$$(4.26) \quad K = \frac{e^{i/2}}{(i\mu_+)} [1 - e^{-ia'}(0) + (-a) - e^{-ia'}(a)] + \frac{-e^{i/2}}{(i\mu_-)} [1 - e^{-ia'}(0) + (-a) - e^{-ia'}(a)],$$

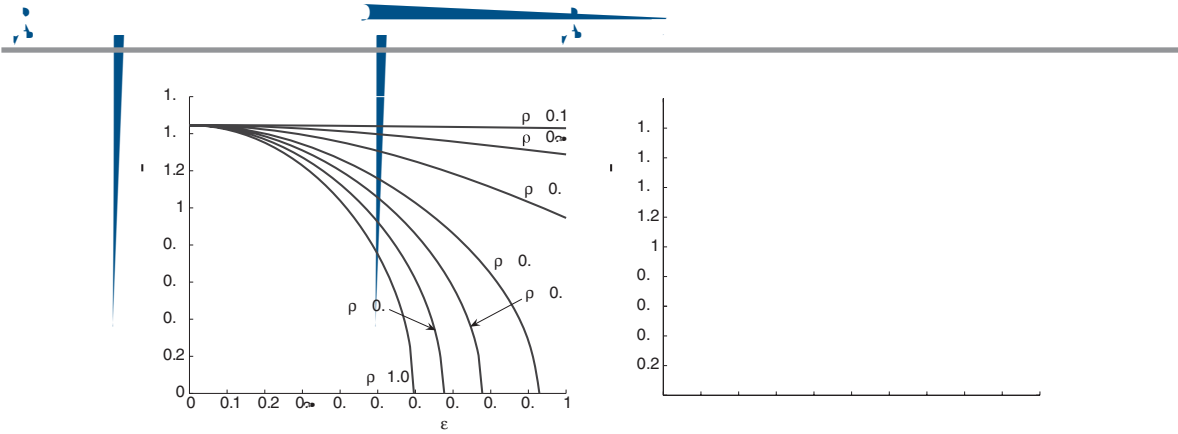
with

$$(4.27) \quad \pm(s) = \int_{-\infty}^{\infty} W(x+s) e^{-\mu_{\pm}x} dx.$$

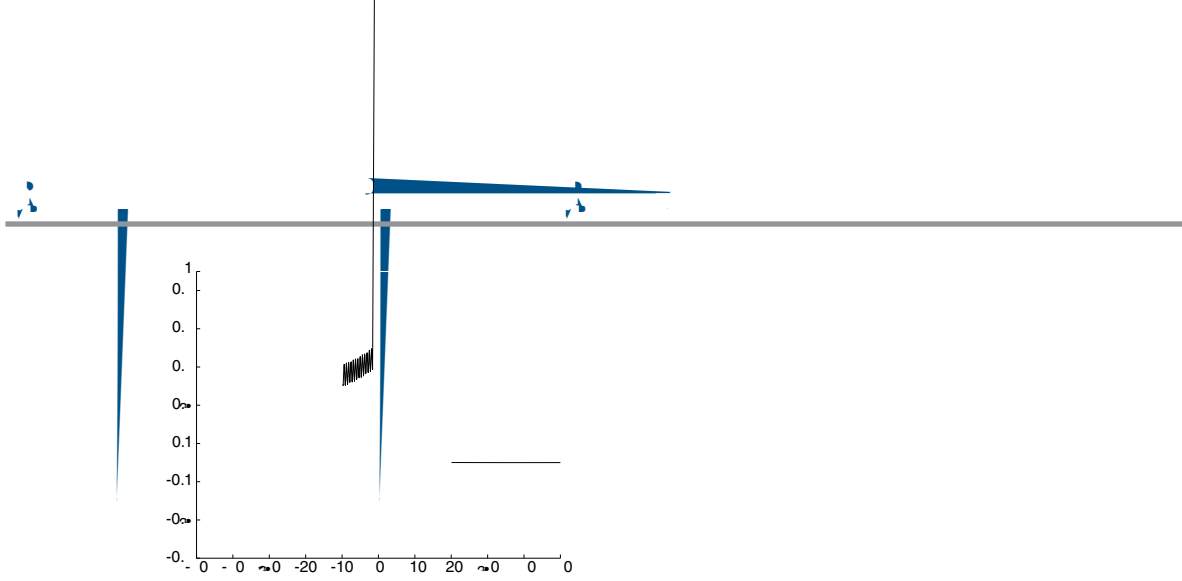
Taking the imaginary part of the above equation then determines the phase function K for $D(x) = \sin(x)$. After a straightforward calculation, we find that

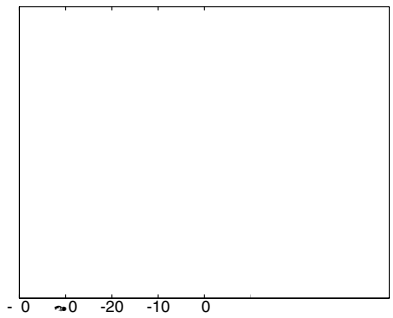
$$(4.28) \quad \frac{K}{2} = (\mu_+ - \mu_-) \sin \frac{-a}{2} + (\mu_+ - \mu_-) \sin \frac{-a}{2} + (\mu_+ - \mu_-) \cos \frac{-a}{2} + (\mu_+ - \mu_-) \cos \frac{-a}{2},$$

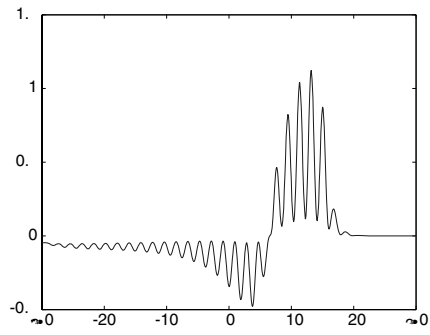
where the explicit expressions for $\mu_{\pm}, \pm, \pm, \pm, \pm$ are given in the appendix.

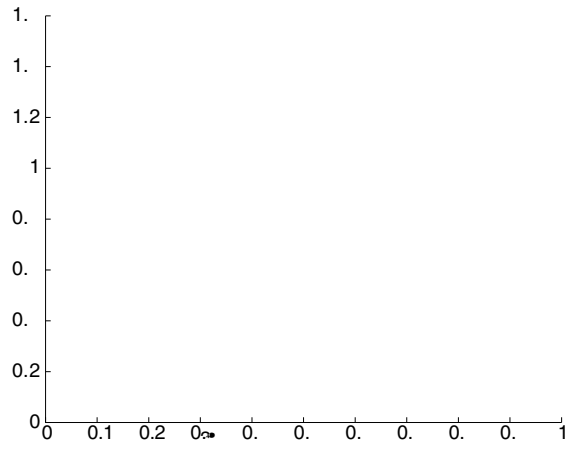


poles, and in general will consist of exponentially small terms. It follows that may be less significant than the $\mathcal{O}(\epsilon)$ terms ignored in the perturbation expansion of (3.4). There-









mm (see Figure 2), whereas waves in slices tend to be only 1 mm wide [31]. More realistic widths and wave speeds could be generated by taking the effective range of synaptic connections to be a few hundred μ m, that is, by assuming that the predominant contribution to synaptic excitability is via local circuitry rather than via long-range patchy horizontal connections. However, inhomogeneities occurring at smaller spatial scales are unlikely to exhibit any periodic structure.

Irrespective of these particular issues, our analysis raises a more general point that would be interesting to pursue experimentally; namely, is it possible to detect the effects of network inhomogeneities by measuring the properties of traveling waves? Signatures of such inhomogeneities would include time-dependent rippling of the wave profile and variations in wave speed. However, such features may not be detectable given the current resolution of microelectrode recordings.

In this appendix we present the explicit parameter-dependent expressions for the various coefficients appearing in the solution of the phase function (4.28). First, the constants premultiplying the periodic functions on the right-hand side of (4.28) are as follows:

$$\begin{aligned}
 \pm &= \frac{\pm}{1 + \mu_{\pm}} \frac{1}{2(1 + \mu_{\pm})} + \frac{1}{2} \frac{e^{-a} - e^{-\mu_{\pm}a}}{\mu_{\pm} - 1} + \frac{e^{-\mu_{\pm}a}}{\mu_{\pm} + 1}, \\
 \pm &= \frac{\pm}{1 + \mu_{\pm}} - \frac{1}{2} \frac{1}{1 + \mu_{\pm}}.
 \end{aligned}$$

$$\begin{aligned}
 & - \int_{-a}^{\infty} [e^{-\mu_+ a} (1 - m_+)] (1 + \dots - (m_- - 1)(1 - m_-)) e^{-\mu_+} \mathcal{M}'_{-}(\cdot) d \\
 & - \int_{-a}^{\infty} [e^{-\mu_- a} (1 - m_-)] (1 - \dots - (1 - m_-)) e^{-\mu_-} \mathcal{M}'_{-}(\cdot) d .
 \end{aligned}$$

The individual integrals can be computed as follows:

$$\int_{-a}^{\infty} e^{-\mu_{\pm}} \mathcal{M}'_{\pm}(\cdot) d = \frac{e^{-a} - 1}{2c(m_+ - m_-)(\mu_{\pm} + 1)} ,$$

$$\int_{-a}^{\infty} e^{-\mu_+} \mathcal{M}'_{-}(\cdot) d = \frac{e^{-a} - 1}{2c(m_+ - m_-)(\mu_- + 1)(\mu_+ + 1)} ,$$

$$\int_{-a}^{\infty} e^{-\mu_-} \mathcal{M}'_{+}(\cdot) d = \frac{e^{-a} - 1}{2c(m_+ - m_-)(\mu_+ + 1)(\mu_- + 1)} ,$$

and

$$\begin{aligned}
 \int_{-a}^{\infty} e^{-\mu_{\pm}} \mathcal{M}'_{\pm}(\cdot) d &= \frac{1}{2c(m_+ - m_-)} \left[\frac{a}{(\mu_{\pm} - 1)} + \frac{1 - e^{\mu_{\pm} - a}}{(\mu_{\pm} - 1)} \right. \\
 &\quad \left. + \frac{e^{-a}(e^{\mu_{\pm} - a} - 1)}{(\mu_{\pm} + 1)} - \frac{a}{2(\mu_{\pm} + 1)} \right] ,
 \end{aligned}$$

$$\begin{aligned}
 \int_{-a}^{\infty} e^{-\mu_+} \mathcal{M}'_{-}(\cdot) d &= \frac{1}{2c(m_+ - m_-)} \left[\frac{1 - e^{-(\mu_- - \mu_+) a}}{(\mu_- - \mu_+)(\mu_- - 1)} - \frac{e^{\mu_+ - a} - 1}{(\mu_+ - 1)(\mu_- - 1)} \right. \\
 &\quad \left. + \frac{e^{\mu_+ a} - e^{-a}}{(\mu_+ + 1)(\mu_-)} \right]
 \end{aligned}$$

-
- [5] C. B. Moore and E. E. Snider, *Front bifurcations in an excitatory neural network*, SIAM J. Appl. Math., 65 (2004), pp. 131–151.
- [6] C. B. Moore, *Pattern formation in visual cortex*, in Methods and Models in Neurophysics, C. C. Chow, B. Gutkin, D. Hansel, C. Meunier, and J. Dalibard, eds., Les Houches Lectures in Neurophysics, Springer-Verlag, Berlin, 2004, pp. 477–574.
- [7] D. C. Moore, A. A. B. C., *Periodicity and directionality in the propagation of excitation in neural network model*, J. Neurophysiol., 60 (1988), pp. 1695–1713.
- [8] B. C. Moore, A. A., *Generation of epileptiform discharge by local circuits of neocortex*, in Epilepsy: Models, Mechanisms and Concepts, P. A. Schwartkroin, ed., Cambridge University Press,

[30] . A. . \uparrow , . A. B , . C. . , . . C. , *Sensorimotor encoding by*